


Investigation Some Nuclear Ground State Properties of the 89Y , $138,139\text{La}$ and $175,176\text{La}$ Rare Earth Elements

Rıdvan Baldık

Zonguldak Bulent Ecevit University, Faculty of Arts and Sciences, Department of Physics, Zonguldak, Turkey,

rbaldik@gmail.com 

Received date: 15.02.2021, Accepted date: 22.04.2021

Abstract

One of the important arguments that will carry today's world to the high technology of the future is the rare earth elements. However, energy will be the most important field in future technology and also, the most important issue in the field will be fusion energy. Of course, in all areas of technology, the rare earth elements will make an important contribution to the development of fusion technology. Also, the nuclear structure of the rare earth elements in nuclear physics has always been the focus of interest and is still a subject that is frequently studied today. Therefore, in this study, nuclear ground-state properties such as the binding energies per particle, the root mean square (rms) charge neutron and proton density radii, the deformation parameters, and the quadrupole moments of the rare earth nuclei as the 89Y , $138,139\text{La}$ and $175,176\text{Lu}$ are calculated by using the Skyrme-Hartree-Fock-Bogolyubov method. The calculations are performed with the HFB9, SIII, SKI3, SKM *, SKO, SKP, SKX, SLY4, SLY5, SLY6, SLY7, UNE0 and UNE1 Skyrme force parameters. Also, the obtained results are discussed and compared with the available experimental data.

Keywords: Skyrme force, nuclear binding energy, deformation parameter, quadrupole moments

89Y , $138,139\text{La}$ ve $175,176\text{La}$ Nadir Toprak Elementlerinin Bazı Nükleer Taban Durum Özelliklerinin Araştırılması

Öz

Günümüz dünyasını gelecekteki yüksek teknolojiye taşıyacak önemli argümanlardan biri nadir toprak elementleridir. Geleceğin teknolojisinde ise en önemli alan enerji olacaktır ve aynı zamanda, bu alanda en önemli konu füzyon enerjisi olacaktır. Elbette, teknolojinin her alanında olduğu gibi, füzyon teknolojisinin gelişimine nadir toprak elementleri de önemli bir katkı sağlayacaktır. Ayrıca, nükleer fizikte nadir toprak elementlerinin nükleer yapısı her zaman ilgi odağı olmuş ve halen günümüzde sıklıkla araştırılan bir konudur. Bu sebeple, bu çalışmada nadir toprak elementleri 89Y , $138,139\text{La}$ ve $175,176\text{Lu}$ çekirdeklerinin parçacık başına bağlanma enerjileri, kare ortalama karekök yük, nötron ve proton yoğunluk yarıçapları, deformasyon parametreleri ve kuadropol momentleri gibi nükleer taban durum özellikleri Skyrme-Hartree-Fock-Bogolyubov metodu kullanılarak hesaplanmıştır. Hesaplamalarda Skyrme kuvvet parametreleri olarak HFB9, SIII, SKI3, SKM*, SKO, SKP, SKX, SLY4, SLY5, SLY6, SLY7, UNE0 and UNE1 kullanılmıştır. Elde edilen sonuçlar mevcut deneysel verilerle kıyaslanmış ve tartışılmıştır.

Anahtar kelimeler: Skyrme kuvveti, nükleer bağlanma enerjisi, deformasyon parametresi, kuadropol moment

INTRODUCTION

The rare earth elements (REEs) are used extensively in the field of technology and will be an important component in the high technology world of the future (Şahiner, Akgök, Arslan, & Ergin, 2017). These elements have wide usage the areas such as clean energy, lasers, microwave filters, camera lenses, nuclear batteries, neutron capture, computer memories, PET (positron emission tomography) scanning detectors (Şahiner et al., 2017). Also, these

elements are important as they make metals stronger, generators more efficient, mobile phones smaller and laptops lighter. The REEs reserves in the world are approximately 36.52% in the People's Republic of China, 19.27% in Russia, 13.19% in the USA, 5.48% in Australia, and 3.14% in India (Şahiner et al., 2017). The rich reserves in terms of REEs in Turkey are Kızılcaören-Eskisehir and Malatya-Kuluncak regions

and the other available REEs reserves have been identified but not operated yet (Şahiner et al., 2017).

The fusion reaction most likely to be used for fusion energy is the deuterium (D) - tritium (T) reaction. Plasma must be formed for this reaction to occur, and this is only possible at very high temperatures (over 100 million degrees). One of the most important problems for the controlled thermonuclear fusion is how the structural materials in the severe environmental conditions due to the high temperature and intense radiation of the fusion medium will perform. These severe conditions cause changes in the surface morphology of the fusion structural materials as bubbling, embrittlement, brittleness, thermal and mechanical properties etc. (Luo et al., 2016). Therefore, the REEs are used to make stronger and more resistant alloys in the fusion structure materials. For example, W (tungsten) and its alloys are considered potential plasma coating materials (Shu, Wakai, & Yamanishi, 2007). In Wurster et al. studies in 2013, they managed to partially change the performance of W through microalloying and doping of dispersed hard particles to produce tungsten-based materials (Wurster et al., 2013). Besides, as a contribution to this study in the literature, it is possible to come across studies in which REEs such as Y, La and Lu are used to increase the performance of tungsten-based material (Liu, Ma, & Huang, 2007; Luo et al., 2016).

Knowing the ground-state properties of the REEs nuclei such as Y, La and Lu, which are used to increase the performance of tungsten-based fusion structural material, is important for the performance of the structural material. Therefore, the ^{89}Y , $^{138,139}\text{La}$ and $^{175,176}\text{Lu}$ REEs nuclei are considered in this study. The natural abundances of these isotopes are 100% for the ^{89}Y , 0.089% for the ^{138}La , 99.911% for the ^{139}La and 97.401% for the ^{175}Lu and 2.599% for the ^{176}Lu . Also, ^{138}La ($T_{1/2} = 103$ Gy) and ^{176}Lu ($T_{1/2} = 37.01$ Gy) nuclei are long half-life radioactive elements, while the others are stable nuclei (Kondev, Wang, Huang, Naimi, & Audi, 2021). Nuclear properties of these nuclei such as the binding energies per particle, the root mean square (rms) charge, neutron and proton density radii, the quadrupole deformation parameters and the quadrupole moments are calculated by using the axially deformed by Skyrme-Hartree-Fock-Bogolyubov (SHFB) method

(Bogolyubov, 1958; Skyrme, 1958). The calculations are performed by the axially deformed solution of the SHFB equations using the harmonic oscillator basis in the *hfbtho* (v3.00) code (Perez, Schunck, Lasserri, Zhang, & Sarich, 2017). In addition, the HFB9, SIII, SKI3, SKM *, SKO, SKP, SKX, SLY4, SLY5, SLY6, SLY7, UNE0 and UNE1 parameter sets have been used as Skyrme force parameters. The obtained findings are compared with the available experimental data in the literature.

MATERIAL AND METHODS

Skyrme-Hartree-Fock-Bogolyubov Method

The nucleus is a many-body problem, and Hartree-Fock (HF) method is one of the basic methods of solving the many-body problem. Also, there are additional correlations between closed shells and unpaired particle in the nucleus. In the Bardeen-Cooper-Schrieffer (BCS) model, the behavior of these correlations are examined in the generalized single particle description defined as quasi-particle (Ring & Schuk, 1980). The Hartree-Fock-Bogolyubov (HFB) theory proposed by Bogolyubov in 1958 (Bogolyubov, 1958) is the combined and generalized version of these two methods. In this theory, which is based on the superfluid model of the nucleus (independent quasi-particle model). When the HFB method, which reduces the multi-particle problem to a set of differential equations, is applied to the zero-range Skyrme force, this method is called the Skyrme-Hartree-Fock-Bogolyubov (SHFB) method. Using the HFB method together with the effective Skyrme force makes it a powerful tool to study the ground-state properties of the nucleus (Bennaceur & Dobaczewski, 2005). The variation method, which aims to find the ground-state energy by minimizing the derivation of the SHFB equations, is used. In the SHFB method, the local energy density function is given as follows;

$$E[\rho, \tilde{\rho}] = \int d^3\vec{r} H(\vec{r}). \quad (1)$$

Here, the ground-state wave function is obtained by minimizing the total energy. The Hamiltonian energy density as the sum of the particle-hole and particle-particle interactions are given as follows (Dobaczewski, Flocard, & Treiner, 1984);

$$H(\vec{r}) = H_{ph}(\vec{r}) + \tilde{H}_{pp}(\vec{r}). \quad (2)$$

Research article/Araştırma makalesi
DOI: 10.29132/ijpas.875700

where $H_{ph}(\vec{r})$ is the particle-hole Hamiltonian and explicit formula;

$$H_{ph}(\vec{r}) = \frac{\hbar^2}{2m} + \frac{1}{2}t_0 \left\{ \left(1 + \frac{x_0}{2}\right) \rho^2 - \left(x_0 + \frac{1}{2}\right) \sum_q \rho_q^2 \right\} + \frac{1}{4}t_1 \left\{ \left(1 + \frac{x_1}{2}\right) \left[\rho \tau - \frac{3}{4}(\vec{\nabla} \rho)^2 \right] - \left(x_1 + \frac{1}{2}\right) \sum_q \left[\rho_q \tau_q + \frac{3}{4}(\vec{\nabla} \rho_q)^2 \right] \right\} + \frac{1}{4}t_2 \left\{ \left(1 + \frac{x_2}{2}\right) \left[\rho \tau - \frac{3}{4}(\vec{\nabla} \rho)^2 \right] - \left(x_2 + \frac{1}{2}\right) \sum_q \left[\rho_q \tau_q + \frac{3}{4}(\vec{\nabla} \rho_q)^2 \right] \right\} - \frac{1}{8}(x_1 t_1 + x_2 t_2) \sum_{ij} [J_{ij}^2] + \frac{1}{8}(t_1 - t_2) \sum_{ij} [J_{ij}^2] + \frac{1}{12}t_3 \rho^\alpha \left\{ \left(1 + \frac{x_1}{2}\right) \rho^2 - \left(x_3 + \frac{1}{2}\right) \sum_q \rho_q^2 \right\} + \frac{1}{2}t_4 \sum_{ijk} \epsilon_{ijk} \left\{ J_{ij} \nabla_k \rho + \sum_q J_{q,ij} \nabla_k \rho_q \right\} \quad (3)$$

Here ρ, τ and J are represented with $\rho = \rho_n + \rho_p$, $\tau = \tau_n + \tau_p$ and $\vec{J} = \vec{J}_n + \vec{J}_p$. Also, $\tilde{H}_{pp}(\vec{r})$ is the particle-particle Hamiltonian as follows;

$$\tilde{H}_{pp}(\vec{r}) = \sum_q \left\{ \frac{1}{4}t_0(1 - x_0) \tilde{\rho}_q^2 - \frac{1}{4}t_1(1 - x_1) \left[\tilde{\rho}_q \tilde{\tau}_q + \frac{1}{4}(\vec{\nabla} \tilde{\rho})^2 \right] + \frac{1}{4}t_2(1 - x_2) \sum_{ij} \tilde{J}_{q,ij}^2 + \frac{1}{2}t_4 \sum_{ij} [\tilde{J}_{q,ii} \tilde{J}_{q,jj} - \tilde{J}_{q,ij} \tilde{J}_{q,ji}] + \frac{1}{24}t_3(1 - x_3) \rho^\alpha \tilde{\rho}^2 \right\} \quad (4)$$

These Hamiltonians are created by using the effective masses, the potential and the spin-orbital potential energies depending on the kinetic densities. The explicit form of the effective mass expression, also called the parameter of inertia, is given as follows:

$$M = \frac{\hbar^2}{2m_q^*} = \frac{\hbar^2}{2m} + \frac{1}{4}t_1 \left\{ \left(1 + \frac{x_1}{2}\right) \rho - \left(x_1 + \frac{1}{2}\right) \rho_q \right\} + \frac{1}{4}t_2 \left\{ \left(1 + \frac{x_2}{2}\right) \rho - \left(x_2 + \frac{1}{2}\right) \rho_q \right\} \quad (5)$$

The pairing effective mass is expressed with

$$\tilde{M} = \frac{1}{4}t_1(1 - x_1) \tilde{\rho}_q, \quad (6)$$

Also, the particle-hole field, namesake as the HF area, is as follows:

$$U = t_0 \left\{ \left(1 + \frac{x_0}{2}\right) \rho - \left(x_0 + \frac{1}{2}\right) \sum_q \rho_q \right\} + \frac{1}{4}t_1 \left\{ \left(1 + \frac{x_1}{2}\right) \left[\tau - \frac{3}{2}(\nabla^2 \rho) \right] - \left(x_1 + \frac{1}{2}\right) \sum_q \left[\tau_q + \frac{3}{2}(\nabla^2 \rho_q) \right] \right\} + \frac{1}{4}t_2 \left\{ \left(1 + \frac{x_2}{2}\right) \left[\tau - \frac{3}{2}(\nabla^2 \rho) \right] - \left(x_2 + \frac{1}{2}\right) \sum_q \left[\tau_q + \frac{3}{2}(\nabla^2 \rho_q) \right] \right\} - \frac{1}{12}t_3 \left\{ \left(1 + \frac{x_3}{2}\right) (2 + \alpha) \rho^{\alpha+1} - \left(x_3 + \frac{1}{2}\right) \left[\alpha \rho^{\alpha-1} \sum_{q'} \rho_{q'}^2 + 2 \rho \rho_{q'} \right] + \frac{1}{2}(1 - x_3) \alpha \rho^{\alpha-1} \sum_{q'} \tilde{\rho}_{q'}^2 \right\} - \frac{1}{2}t_4 \sum_{ijk} \epsilon_{ijk} \nabla_k [J_{ij} + J_{q,ij}]. \quad (7)$$

The particle-particle field is given as;

$$\tilde{U} = \frac{1}{2}t_0(1 - x_0) \tilde{\rho}_q + \frac{1}{4}t_1(1 - x_1) \left[\tau_q - \frac{1}{2}(\nabla^2 \tilde{\rho}_q) \right] + \frac{1}{12}t_3(1 - x_3) \rho^\alpha \tilde{\rho}_q, \quad (8)$$

The fields representing particle and pairing spin-orbit interaction are given as follows, respectively;

$$W = -\frac{1}{4}(x_1 t_1 + x_2 t_2) J + \frac{1}{8}(t_1 - t_2) J_q + t_4 \nabla(\rho + \rho_q), \quad (9)$$

$$\tilde{W} = \left[-\frac{1}{2}t_2(I + x_2) J + t_4 \right] \tilde{J}_q. \quad (10)$$

To obtain the Schrödinger equation for the SHFB method, these fields are written in matrix form as follows:

$$M = \begin{pmatrix} M & M \\ \tilde{M} & \tilde{M} \end{pmatrix}, \quad U = \begin{pmatrix} U - E_f & \tilde{U} \\ \tilde{U} & -U + E_f \end{pmatrix} \quad (11)$$

and

$$U_{so} = \begin{pmatrix} W & \tilde{W} \\ \tilde{W} & W \end{pmatrix}. \quad (12)$$

The Schrödinger equation is expressed in the coordinate space using these matrices (Bennaceur & Dobaczewski, 2005):

$$\left[-\frac{d}{dr} M \frac{d}{dr} + U + M \frac{\ell(\ell+1)}{r^2} + U_{so} \right] \begin{pmatrix} \phi_1 \\ \phi_1 \end{pmatrix} = E \begin{pmatrix} \phi_1 \\ \phi_1 \end{pmatrix}. \quad (13)$$

The solution of the SHFB differential equation is done by using the HF iteration. With this iteration, when the optimum wave function is obtained, the nuclear ground-state properties are calculated. The rms charge and nucleon densities are calculated by using this wave function and the rms charge, neutron and proton density radii are obtained by using the densities. Lastly, the quadrupole moments and the deformation parameter are calculated using the following expressions, respectively (Stoitsov, Dobaczewski, Nazarewicz, & Ring, 2005);

$$\hat{Q} = 2Z^2 - r^2 \quad (14)$$

$$\beta = \sqrt{\frac{\pi \langle \hat{Q} \rangle}{5 \langle r^2 \rangle}}. \quad (15)$$

The HFBTHOv3.00 Code

The HFBTHO code performs the HFB equation on the harmonic oscillator basis. The first version HFBTHOv1.66 code was only solved for even-even nuclei using Skyrme effective force in the particle-hole channel and also, the axial quadrupole deformations (Stoitsov et al., 2005). In the second version was the HFBTHOv2.00d code, which included to solves of odd-even and odd-odd nuclei and the calculation of axial multipole moments of a nucleus (Stoitsov et al., 2013). The most important modifications of the last version HFBTHOv3.00 code solves the HFB equation for both the particle-hole and particle-particle channel and also uses Gogny force as another effective force option (Perez et al., 2017). Also, the code contains a small fission toolkit for the charge, mass and deformations of the fission fragments.

RESULTS AND DISCUSSION

In this study, the binding energies per particle, the rms charge, neutron and proton density radii, the deformation parameters and the quadrupole moments are calculated by using the Hartree-Fock-Bogolyubov method with Skyrme forces for some fusion structural materials as the ^{89}Y , $^{138,139}\text{La}$ ve $^{175,176}\text{Lu}$ nuclei. The calculated binding energy per particle using different Skyrme force parameter and their comparison with experimental data (Vasil'evich et al., 2021) are presented in Table 1. According to the results, the obtained binding energies per particle

using the HFB9 parameter set for the ^{89}Y and $^{138,139}\text{La}$ nuclei, and the SKX parameter for the $^{175,176}\text{Lu}$ nuclei are in agreement with the experimental data.

The obtained rms charge density radii using the SHFB method for different Skyrme force parameters are rather close to each other and, the theoretical rms charge radii are also obtained to be in good agreement with the experimental data (Table 2). These results show that the predictions of the rms charge density radii with the SHFB method for the REEs in this study are substantially effective. Also, for the theoretical rms charge density radii closest to the experimental data (Vasil'evich et al., 2021), the Skyrme interactions are the SKX for the ^{89}Y and ^{139}La nuclei, the SKO for the ^{138}La nucleus and the SIII for the $^{175,176}\text{Lu}$ nuclei.

The results of rms neutron and proton density radii for the ^{89}Y , $^{138,139}\text{La}$ and $^{175,176}\text{Lu}$ nuclei are presented in Table 3. The obtained results using the SHFB method are not compared with the experimental data, because of unavailable experimental data in the literature. The values of the rms neutron density radii for the SIII and SKO parameter sets of the ^{89}Y nucleus, for the SKI3 parameter set of the $^{138,139}\text{La}$, and $^{175,176}\text{Lu}$ nuclei are bigger than those for the other Skyrme force parameters in this study. On the other hand, the theoretical rms proton density radii of the SIII parameter set of the ^{89}Y , $^{138,139}\text{La}$ and $^{175,176}\text{Lu}$ nuclei in this study are bigger than those of the other Skyrme force parameters.

The obtained deformation parameters and the quadrupole moments, and the available experimental data (Vasil'evich et al., 2021) for the ^{89}Y , $^{138,139}\text{La}$ and $^{175,176}\text{Lu}$ nuclei are presented in Table 4 and 5. Between the REEs nuclei considered in this study, only, the experimental data of these quantities for the ^{89}Y nucleus are not available in the literature. The shape of the nucleus, according to calculated deformation parameters using the thirteen Skyrme force parameters, may be prolate for the SIII, SKO, SKP and UNE1 or oblate for the other Skyrme parameter sets. Also, while the values of deformation parameters of the ^{89}Y nucleus for the prolate shape are changed in between 0.010-0.057, it ranges from -0.016 to -0.086 for the oblate. Besides, according to the obtained deformation parameters, the ^{89}Y nucleus has a small deformation. On the other hand, for the ^{138}La nucleus, the calculated deformation parameter using the SKI3 parameter set is the closest to the

Research article/Araştırma makalesi
DOI: 10.29132/ijpas.875700

experimental data. Also, the obtained deformation parameters using the SIII, SKM*, SKX and SLY6 sets for the ^{139}La nucleus have the same value (0.006), and the value is the closest to the experimental data. The theoretical results for the $^{138-139}\text{La}$ isotopes have small deformations like the ^{89}Y nucleus. Among the results of the deformation parameter for the $^{175-176}\text{Lu}$ isotopes, the closest Skyrme interactions to the experimental data are the UNE0 and SKX, respectively. Also, according to the deformation parameters for these isotopes, it is seen that these nuclei deviate significantly from the spherical shape.

The experimental data of the quadrupole moment for the ^{89}Y nucleus is not available in the

literature. While the obtained quadrupole moments using the SIII, SKO, SKP and UNE1 Skyrme interactions for the nucleus have positive values, those for the other Skyrme interactions in this study have negative values (Table 5). For the $^{138,139}\text{La}$ isotopes, the calculated quadrupole moments using the SLY6 and SLY4 Skyrme interactions, respectively, are in agreement with the experimental data. In the case of the $^{175,176}\text{Lu}$ isotopes, the theoretical quadrupole moments for UNE0 and SKP Skyrme interactions, respectively, are compatible with the experimental data.

Table 1. The calculated binding energy per particle (in MeV) using the Skyrme force parameters for the ^{89}Y , $^{138,139}\text{La}$ and $^{175,176}\text{Lu}$ nuclei. The experimental data are taken from ref. (Vasil'evich et al., 2021).

Parameter Set	^{89}Y	^{138}La	^{139}La	^{175}Lu	^{176}Lu
HFB9	8.705	8.361	8.372	7.93	7.917
SIII	8.649	8.304	8.317	7.869	7.859
SKI3	8.593	8.284	8.299	7.834	7.845
SKM*	8.674	8.322	8.335	7.886	7.874
SKO	8.571	8.267	8.270	7.887	7.884
SKP	8.667	8.315	8.333	7.960	7.954
SKX	8.931	8.546	8.551	8.137	8.143
SLY4	8.682	8.320	8.331	7.876	7.862
SLY5	8.644	8.272	8.313	7.870	7.856
SLY6	8.596	8.274	8.287	7.844	7.829
SLY7	8.576	8.264	8.273	7.845	7.830
UNE0	8.672	8.345	8.349	7.980	7.968
UNE1	8.689	8.323	8.349	7.951	7.934
Experiment	8.714	8.375	8.378	8.069	8.059

Table 2. The calculated rms charge density radii (in fm) using the Skyrme force parameters for the ^{89}Y , $^{138,139}\text{La}$ and $^{175,176}\text{Lu}$ nuclei. The experimental data are taken from ref. (Vasil'evich et al., 2021).

Parameter Set	^{89}Y	^{138}La	^{139}La	^{175}Lu	^{176}Lu
HFB9	4.279	4.871	4.875	5.265	5.271
SIII	4.316	4.936	4.940	5.324	5.331

SKI3	4.252	4.859	4.863	5.247	5.262
SKM*	4.280	4.868	4.868	5.255	5.263
SKO	4.238	4.847	4.850	5.255	5.267
SKP	4.300	4.878	4.884	5.271	5.283
SKX	4.248	4.849	4.855	5.244	5.266
SLY4	4.289	4.878	4.883	5.277	5.279
SLY5	4.285	4.869	4.872	5.266	5.271
SLY6	4.285	4.877	4.885	5.276	5.282
SLY7	4.290	4.884	4.889	5.278	5.290
UNE0	4.268	4.854	4.858	5.255	5.260
UNE1	4.262	4.865	4.873	5.263	5.271
Experiment	4.243	4.847	4.855	5.37	5.374

Table 3. The calculated rms neutron and proton density radii (in fm) using the Skyrme force parameters for the ^{89}Y , $^{138,139}\text{La}$ and $^{175,176}\text{Lu}$ nuclei.

Parameter Set	The rms neutron density radii					The rms proton density radii				
	^{89}Y	^{138}La	^{139}La	^{175}Lu	^{176}Lu	^{89}Y	^{138}La	^{139}La	^{175}Lu	^{176}Lu
HFB9	4.279	4.922	4.933	5.332	5.344	4.202	4.805	4.809	5.205	5.211
SIII	4.302	4.957	4.967	5.361	5.373	4.239	4.871	4.875	5.264	5.272
SKI3	4.291	4.961	4.974	5.375	5.396	4.174	4.793	4.798	5.187	5.201
SKM*	4.280	4.928	4.935	5.335	5.349	4.203	4.803	4.802	5.195	5.203
SKO	4.302	4.957	4.970	5.367	5.388	4.160	4.781	4.784	5.195	5.207
SKP	4.295	4.925	4.937	5.330	5.347	4.224	4.812	4.819	5.210	5.223
SKX	4.257	4.903	4.916	5.307	5.333	4.170	4.783	4.789	5.184	5.206
SLY4	4.286	4.929	4.940	5.350	5.359	4.212	4.812	4.817	5.217	5.219
SLY5	4.285	4.927	4.934	5.342	5.352	4.208	4.803	4.807	5.206	5.211
SLY6	4.283	4.928	4.941	5.347	5.358	4.208	4.812	4.819	5.216	5.222
SLY7	4.291	4.935	4.946	5.349	5.365	4.213	4.818	4.823	5.218	5.230
UNE0	4.301	4.938	4.952	5.345	5.361	4.190	4.787	4.793	5.194	5.200
UNE1	4.281	4.937	4.950	5.343	5.358	4.184	4.799	4.807	5.203	5.211

Table 4. The calculated quadrupole deformation parameters (β) using the Skyrme force parameters for the ^{89}Y , $^{138,139}\text{La}$ and $^{175,176}\text{Lu}$ nuclei. The experimental data are taken from ref. (Vasil'evich et al., 2021).

Parameter Set	^{89}Y	^{138}La	^{139}La	^{175}Lu	^{176}Lu
HFB9	-0.062	0.031	0.002	0.003	0.009

SIII	0.021	0.009	0.006	0.004	0.005
SKI3	-0.074	0.034	0.004	0.005	0.098
SKM*	-0.080	0.068	0.006	0.002	0.002
SKO	0.010	0.055	0.003	0.004	0.083
SKP	0.057	0.006	0.005	0.013	0.081
SKX	-0.016	0.005	0.006	0.003	0.131
SLY4	-0.082	0.014	0.005	0.003	0.003
SLY5	-0.086	0.004	0.004	0.001	0.004
SLY6	-0.078	0.011	0.006	0.002	0.006
SLY7	-0.082	0.019	0.005	0.002	0.007
UNE0	-0.031	0.028	0.005	0.073	0.066
UNE1	0.016	0.017	0.004	0.009	0.019
Experiment	-	0.043 0.044	0.024	0.292 0.303	0.286 0.289 0.295

Table 5. The calculated quadrupole moments (Q) (in b) using the Skyrme force parameters for the ^{89}Y , $^{138,139}\text{La}$ and $^{175,176}\text{Lu}$ nuclei. The experimental data are taken from ref. (Vasil'evich et al., 2021).

Parameter Set	^{89}Y	^{138}La	^{139}La	^{175}Lu	^{176}Lu
HFB9	-1.264	1.299	0.098	0.163	0.586
SIII	0.439	0.399	0.239	0.28	0.295
SKI3	-1.488	1.433	0.157	0.311	6.143
SKM*	-1.614	2.818	0.234	0.098	0.134
SKO	0.207	2.292	0.137	0.223	5.183
SKP	1.17	0.252	0.227	0.804	5.069
SKX	-0.322	0.215	0.247	0.186	8.104
SLY4	-1.661	0.598	0.198	0.169	0.211
SLY5	-1.742	0.152	0.169	0.075	0.267
SLY6	-1.583	0.441	0.255	0.151	0.355
SLY7	-1.666	0.796	0.225	0.107	0.45
UNE0	-0.624	1.168	0.226	4.518	4.086
UNE1	0.331	0.687	0.172	0.582	1.179
Experiment	-	0.430 0.450	0.200	3.490 3.620	4.920 4.970 5.070

SUMMARY AND CONCLUSION

In this study, some ground nuclear properties such as the binding energies per particle, the rms charge, neutron and proton density radii, the deformation parameters, the quadrupole moments of the ^{89}Y , $^{138,139}\text{La}$ and $^{175,176}\text{Lu}$ REEs nuclei, which are important for the fusion structural material

performance are calculated using the SHFB method and compared with the available experimental data.

For the binding energies per particle, the HFB9 Skyrme interaction for the ^{89}Y , $^{138,139}\text{La}$ nuclei and the SKX Skyrme interaction for the $^{175,176}\text{Lu}$ nuclei are the optimal parameter sets. Also, the best of the Skyrme parameters for the theoretical rms charge

Research article/Araştırma makalesi
 DOI: 10.29132/ijpas.875700

density radii are the SKX for the ^{89}Y and ^{139}La nuclei, the SKO for the ^{138}La nucleus, and the SIII for the $^{175,176}\text{Lu}$ isotopes. In addition, the axially deformed SHFB method using the harmonic oscillator basis is a very effective on the rms charge density radii the considered REEs in this study. On the other hand, the experimental data for the rms neutron and proton density radii for the ^{89}Y , $^{138,139}\text{La}$ and $^{175,176}\text{Lu}$ nuclei are not available in the literature, thus no comparison could be made between the theoretical results and experimental data. Therefore, since the rms neutron and proton density radii of these REEs are not previously calculated, these results will contribute to the literature.

According to the deformation parameter results, it was concluded that there is a small deformation for the ^{89}Y , $^{138,139}\text{La}$ nuclei, and a large deformation for $^{175,176}\text{Lu}$ isotopes. On the other hand, the obtained quadrupole moment results using the SHFB method are closer to the experimental data than the results of the deformation parameter. Also, as it is known, the extremely large quadrupole moments with a few barns are quite difficult to theoretically predict. Therefore, the prediction of the $^{175,176}\text{Lu}$ nuclei with the extremely large quadrupole moments via the SHFB method is quite successful.

According to the results of this study, one of the Skyrme interactions is not only sufficient to explain all ground-state properties of the nucleus. The reason is that each Skyrme parameter set is adjusted to the different theoretical or experimental properties of the nuclei, so one of the parameter sets is not successful alone. Also, the results of this study can be used for better understanding the nuclear structure of the REE nuclei such as the ^{89}Y , $^{138,139}\text{La}$ and $^{175,176}\text{Lu}$.

CONFLICT OF INTEREST

The Author report no conflict of interest relevant to this article

RESEARCH AND PUBLICATION ETHICS STATEMENT

The author declares that this study complies with research and publication ethics.

REFERENCES

Audi, G., Kondev, F. G., Wang, M., Pfeiffer, B., Blachot, J., Sun, X., & MacCormick, M. (2012). NUBASE2012 Evaluation of Nuclear Properties. *Chinese Physics C*, 36(12), 1157–1286. <https://doi.org/10.1016/j.nds.2014.06.127>

- Bennaceur, K., & Dobaczewski, J. (2005). Coordinate-space solution of the Skyrme-Hartree-Fock-Bogolyubov equations within spherical symmetry. the program HFBRAD (v1.00). *Computer Physics Communications*, 168(2), 96–122. <https://doi.org/10.1016/j.cpc.2005.02.002>
- Bogolyubov, N. N. (1958). On a Variational Principle in the Many Body Problem. *Sov. Phys. Dokl.*, 3, 292–294.
- Dobaczewski, J., Flocard, H., & Treiner, J. (1984). Hartree-Fock-Bogolyubov description of nuclei near the neutron-drip line. *Nuclear Physics, Section A*, 422(1), 103–139. [https://doi.org/10.1016/0375-9474\(84\)90433-0](https://doi.org/10.1016/0375-9474(84)90433-0)
- Liu, W. S., Ma, Y. Z., & Huang, B. Y. (2007). Investigation of fracture failure and strengthening-toughening of tungsten-based alloys. *Powder Metallurgy Industry*, 17(4), 26–31.
- Luo, L., Shi, J., Lin, J., Zan, X., Zhu, X., Xu, Q., & Wu, Y. (2016). Microstructure and performance of rare earth element-strengthened plasma-facing tungsten material. *Scientific Reports*, 6(March), 1–9. <https://doi.org/10.1038/srep32701>
- Perez, R. N., Schunck, N., Lasserri, R. D., Zhang, C., & Sarich, J. (2017). Axially deformed solution of the Skyrme-Hartree-Fock-Bogolyubov equations using the transformed harmonic oscillator basis (III) HFBRAD (v3.00): A new version of the program. *Computer Physics Communications*, 220(March 2018), 363–375. <https://doi.org/10.1016/j.cpc.2017.06.022>
- Ring, P., & Schuck, P. (1980). *The Nuclear Many Body Problem*.
- Şahiner, M., Akgök, Y. Z., Arslan, M., & Ergin, M. H. (2017). *Dünyada ve Türkiye’de Nadir Toprak Elementleri*. Ankara, Turkey.
- Shu, W. ., Wakai, E., & Yamanishi, T. (2007). Blister bursting and deuterium bursting release from tungsten exposed to high fluences of high flux and low energy deuterium plasma. *Nuclear Fusion*, 47(3), 201–209. <https://doi.org/10.1088/0029-5515/47/3/006>
- Skyrme, T. H. R. (1958). The effective nuclear potential. *Nuclear Physics*, 9(4), 615–634. [https://doi.org/10.1016/0029-5582\(58\)90345-6](https://doi.org/10.1016/0029-5582(58)90345-6)
- Stoitsov, M. V., Dobaczewski, J., Nazarewicz, W., & Ring, P. (2005). Axially deformed solution of the Skyrme-Hartree-Fock-Bogolyubov equations using the transformed harmonic oscillator basis. the program HFBRAD (v1.66p). *Computer Physics*

Research article/Araştırma makalesi
DOI: 10.29132/ijpas.875700

Communications, 167(1), 43–63.
<https://doi.org/10.1016/j.cpc.2005.01.001>

Stoitsov, M. V., Schunck, N., Kortelainen, M., Michel, N., Nam, H., Olsen, E., ... Wild, S. (2013). Axially deformed solution of the Skyrme-Hartree-Fock-Bogoliubov equations using the transformed harmonic oscillator basis (II) hfbtho v2.00d: A new version of the program. *Computer Physics Communications*, 184(6), 1592–1604.
<https://doi.org/10.1016/j.cpc.2013.01.013>

Vasil'evich, V. V., Evgen'evich, S. M., Sergeevich, R. D., Vladimirovich, C. V., Nickolaevich, P. N., Yur'evich, K. S., & Valery, V. V. (2021). Centre for Photonuclear Experiments Data.

Wurster, S., Baluc, N., Battabyal, M., Crosby, T., Du, J., García-Rosales, C., ... Pippan, R. (2013). Recent progress in R&D on tungsten alloys for divertor structural and plasma facing materials. *Journal of Nuclear Materials*, 442(1-3 SUPPL.1), S181–S189.
<https://doi.org/10.1016/j.jnucmat.2013.02.074>